

Selective modification of the $\text{Er}^{3+} {}^4I_{11/2}$ branching ratio by energy transfer to Eu^{3+}

C. Strohhöfer,^{a)} P. G. Kik, and A. Polman

FOM Institute for Atomic and Molecular Physics, Kruislaan 407, 1098 SJ Amsterdam, The Netherlands

(Received 6 March 2000; accepted for publication 24 July 2000)

We present an investigation of Er^{3+} photoluminescence in Y_2O_3 waveguides codoped with Eu^{3+} . As a function of europium concentration we observe an increase in decay rate of the erbium ${}^4I_{11/2}$ energy level and an increase of the ratio of photoluminescence emission from the ${}^4I_{13/2}$ and ${}^4I_{11/2}$ states. Using a rate equation model, we show that this is due to an energy transfer from the ${}^4I_{11/2} \rightarrow {}^4I_{13/2}$ transition in erbium to europium. This increases the branching ratio of the ${}^4I_{11/2}$ state towards the ${}^4I_{13/2}$ state and results in a higher steady state population of the first excited state of erbium. Absolute intensity enhancement of the ${}^4I_{13/2}$ emission is obtained for europium concentrations between 0.1 and 0.3 at. %. In addition, the photoluminescence due to upconversion processes originating from the ${}^4I_{11/2}$ state is reduced. Using such state-selective energy transfer the efficiency of erbium doped waveguide amplifiers can be increased. © 2000 American Institute of Physics. [S0021-8979(00)01321-9]

I. INTRODUCTION

Erbium-doped optical amplifiers operate at 1540 nm by stimulated emission from the ${}^4I_{13/2}$ state in Er^{3+} . The standard in telecommunications to excite this energy level is via the second excited state ${}^4I_{11/2}$ using 980 nm radiation (cf. Fig. 1). An important ingredient in this pumping scheme is the nonradiative transition between the ${}^4I_{11/2}$ and ${}^4I_{13/2}$ states. Its rate depends on the host material. Incidentally, the most promising materials for erbium doped waveguide amplifiers possess low phonon energies, and therefore small nonradiative transition rates. This is a severe problem, since it gives rise to a significant steady state population of the ${}^4I_{11/2}$ level. As a result, a considerable fraction of Er^{3+} is not available for stimulated emission from the ${}^4I_{13/2}$ state. Moreover, when the ${}^4I_{11/2}$ population is high, excited state absorption and cooperative upconversion processes lead to unwanted excitation of even higher lying energy levels. For these reasons it is desirable to increase the transition rate between the ${}^4I_{11/2}$ and ${}^4I_{13/2}$ energy levels without affecting the optimized properties of the ${}^4I_{13/2}$ state itself. This will make the excitation stored in the ${}^4I_{11/2}$ state available for amplification of 1540 nm radiation, and in the process will also significantly reduce the probability of cooperative upconversion and excited state absorption from the ${}^4I_{11/2}$ state.

One way to enhance the transition rate from the second to the first excited state is engineering the crystal field of the host matrix at the position of the erbium ions. A simpler and newer approach, while leaving the well-established properties of existing waveguide materials unchanged, consists of selectively stimulating the transition between second and first excited state of Er^{3+} by resonant energy transfer to a suitable codopant. Hereby the energy difference between the relevant states of the erbium is transferred to the codopant.

Mainly Ce^{3+} has been investigated as codopant so far,¹⁻³ while Eu^{3+} and Tb^{3+} have been suggested.⁴

In this article we describe codoping of $\text{Er}^{3+}:\text{Y}_2\text{O}_3$ with Eu^{3+} . Yttrium oxide has already proven its suitability for optical amplification in waveguides,⁵ thanks to its high refractive index which provides both a high erbium emission cross section and the possibility of integration on a small area. We investigate the energy transfer by studying the erbium photoluminescence intensities and decay rates as a function of europium concentration, and establish a model based on rate equations which reproduces the data. Finally we show that the green upconversion emission of erbium in a planar waveguide is significantly reduced upon codoping with Eu^{3+} .

II. EXPERIMENT

The samples used in this study were prepared by sputter deposition of Y_2O_3 on a 3- μm -thick thermally grown silicon oxide buffer layer.⁶ Since Y_2O_3 has a higher index of refraction (1.7 at 1500 nm)⁶ than SiO_2 , this structure acts as a planar waveguide. The films are 800 nm thick as determined using Rutherford backscattering spectrometry (RBS). They were doped with erbium by ion implantation at a series of energies between 200 and 500 keV to obtain a flat concentration profile ranging from 30 to 100 nm below the surface. Subsequently europium was implanted into the sample, creating a flat concentration profile that overlaps the erbium doped region completely. By implanting only part of the sample with europium we kept an on-wafer reference of only erbium doped Y_2O_3 . In this way variations in luminescent properties caused by slight differences of quality and treatment between samples can be taken into account. Exact concentrations were determined by RBS analysis and amount to 0.19 at. % erbium and to 0.024, 0.048, 0.12, 0.24, and 0.48

^{a)}Electronic mail: C.Strohhofe@amolf.nl

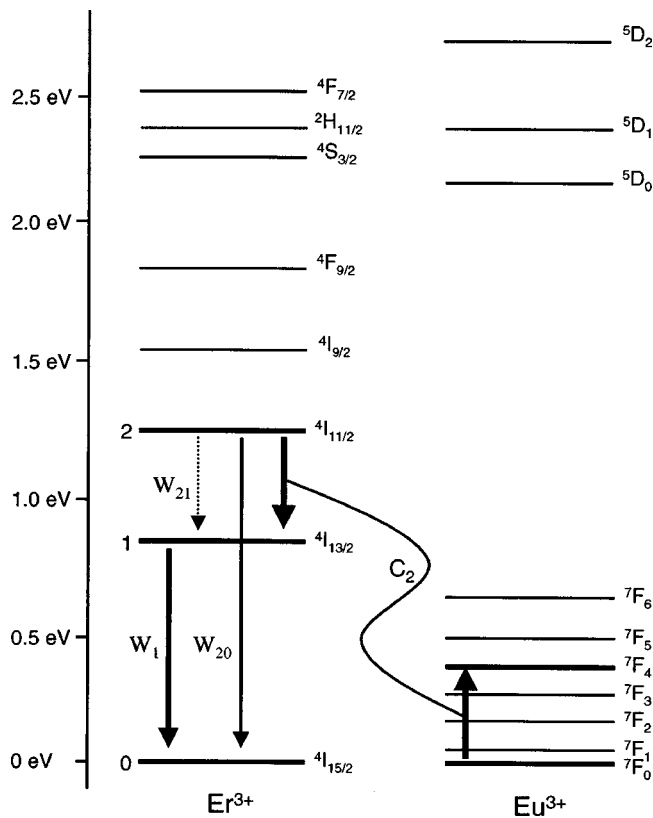


FIG. 1. Energy level diagram of Er^{3+} and Eu^{3+} . Included are the relevant transitions for the rate equation model.

at. % europium. After implantation, the samples were heat treated at 700 °C for 30 min in a rapid thermal annealer under oxygen flow.

For photoluminescence measurements we exploited the planar waveguide geometry of the samples. The 488 nm emission line of an Ar^+ laser was mechanically chopped and then butt coupled into the waveguide via an optical fiber. Photoluminescence emission was collected perpendicular to the waveguide by a multimode fiber with 800 μm core diameter. The signal was dispersed in a 96 cm monochromator. The Er^{3+} emission around 1540 nm was analyzed with a germanium detector cooled to 77 K. For all emission lines with wavelengths shorter than 1100 nm an AgOCs photomultiplier tube was used. The detector signal was fed through a lock-in amplifier. Photoluminescence decay traces of the Er^{3+} emission around 1540 nm were obtained using a digital oscilloscope, averaging typically 2500 single traces. The photoluminescence decay of the 980 nm emission of Er^{3+} , as well as of other emission lines at shorter wavelengths, was measured using a photon counting system and a multichannel scaler.

The 488 nm radiation leaving the planar waveguide at the output end served to trigger lock-in amplifier, oscilloscope, and multichannel scaler. In that way variations of the chopping speed will not have an influence on the accuracy of the measurements.

To obtain a good measure for the intensity ratio of the emission originating from the $^4I_{13/2}$ and $^4I_{11/2}$ levels, spectra were taken of the corresponding lines around 1538 and 980

nm with the cooled germanium detector, taking care not to change the experimental settings. After correction for the detector response, the total intensity in each line was determined by integrating over the spectra.

In order for the analysis presented in this article to be correct, it is important to perform all measurements in a regime where no saturation of the emission signal due to high pump power takes place. Therefore the pump power dependence of the emission line intensity was monitored before each measurement, and the excitation power adjusted to a value within its region of linearity.

III. RESULTS AND DISCUSSION

A. Rate equation model

Figure 1 shows the mechanism we investigated to accelerate the decay rate of the second excited state of Er^{3+} . The rates W_1 , W_{20} , and W_{21} are defined as transition rates of the excited states of Er^{3+} in Y_2O_3 when no codoping with europium has taken place: W_1 is the total decay rate from the $^4I_{13/2}$ level, and is the sum of a radiative rate W_{1r} and a nonradiative rate W_{1nr} . W_{21} is the transition rate between the $^4I_{11/2}$ and $^4I_{13/2}$ states. It consists as well of a nonradiative and a radiative part, this distinction is however unnecessary for the model. W_{20} is the transition rate from the $^4I_{11/2}$ state to the ground state and is taken to be purely radiative. The total decay rate of the $^4I_{11/2}$ state is given by $W_2 = W_{21} + W_{20}$, in the absence of Eu^{3+} . The coupling of the $^4I_{11/2} \rightarrow ^4I_{13/2}$ transition with the Eu^{3+} ion is described by the rate constant C_2 . We assume that an excited Eu^{3+} ion relaxes nonradiatively and fast to its ground state via the 7F_j ladder. This is a reasonable conjecture since the energy level spacings of the 7F_j multiplet of Eu^{3+} in Y_2O_3 can be bridged by two phonons or less of the Y_2O_3 host (highest phonon density of states at 400 cm^{-1}).⁸

This idealized model is complicated by undesirable interactions, which are not depicted in Fig. 1. Important are interactions especially of the $^4I_{13/2}$ state of Er^{3+} with Eu^{3+} (e.g., phonon-assisted energy transfer) or with defects originating from the europium implantation. These constitute additional decay channels for the $^4I_{13/2}$ state. We take this into account by an interaction rate S_1 , which may depend on europium concentration. The rate equations for the population of the excited erbium levels thus have the following form:

$$\begin{aligned} \frac{dN_2}{dt} &= R_2 - W_2 N_2 - C_2 N_q N_2, \\ \frac{dN_1}{dt} &= R_1 - W_1 N_1 + W_{21} N_2 + C_2 N_q N_2 - S_1 N_1. \end{aligned} \tag{1}$$

The symbols R_1 and R_2 signify the excitation rate per unit volume into the first and second excited states of Er^{3+} , respectively. Here we take into account that in the experiments Er^{3+} is initially excited into the $^4F_{7/2}$ state, from which the two lowest levels are fed according to some branching ratio. It is assumed that no excitation-induced saturation of the Er^{3+} occurs, and that the population of the Er^{3+} energy levels is small enough to neglect nonlinear processes such as

cooperative upconversion. N_q represents the concentration of Eu^{3+} . We assume that only an insignificant part of the Eu^{3+} is excited at any time.

The fraction of the population of the ${}^4I_{11/2}$ state that is de-excited via energy transfer to Eu^{3+} , so to speak the branching ratio of the energy transfer, is determined by the ratio of the energy transfer rate and the total decay rate of the $\text{Er}^{3+} {}^4I_{11/2}$ state at a given Eu^{3+} concentration

$$Q_2 = \frac{C_2 N_q}{W_2 + C_2 N_q}. \quad (2)$$

Similarly, we can write the fraction of the population of the ${}^4I_{13/2}$ level that is quenched by the presence of Eu^{3+} or defects caused by the europium implantation as

$$Q_1 = \frac{S_1}{W_1 + S_1}. \quad (3)$$

The branching ratios Q_1 and Q_2 are experimentally accessible via decay rate measurements, as will be shown in the next section. They do not depend on erbium concentration. We would like to draw attention to the differences in definition between Q_1 and Q_2 . The interaction that quenches the first excited state of erbium (S_1) may depend on N_q in an unspecified way, while we assume a dependence of Q_2 on N_q as given by an energy transfer towards europium. In this way we include the possibility that the reduction in luminescence efficiency of the first excited state is caused by defects from the europium implantation, which are not annealed out during the heat treatment. On the other hand the model stays sufficiently precise with respect to the energy transfer from the $\text{Er}^{3+} {}^4I_{11/2}$ level to Eu^{3+} to be tested by experiment.

The ratio of the emission intensities from the ${}^4I_{13/2}$ and ${}^4I_{11/2}$ levels can serve as an independent way to test the model. Substituting Q_1 and Q_2 into the rate Eq. (1) at steady state, and writing the intensities as $I_1 = W_{1r} \cdot h\nu_1 \cdot N_1$ and $I_2 = W_{2r} \cdot h\nu_2 \cdot N_2$ for the emission from the first and second excited states of Er^{3+} , respectively, the intensity ratio is given by the expression

$$\frac{I_1}{I_2} = \frac{1 - Q_1}{1 - Q_2} \frac{I_1^0}{I_2^0} + \frac{W_{1r}}{W_1} \frac{Q_2(1 - Q_1)}{1 - Q_2} \frac{\nu_1}{\nu_2}. \quad (4)$$

I_1 and I_2 are the emission intensities from the first and second excited states of erbium, respectively, in the presence of europium, ν_1 and ν_2 the corresponding emission frequencies, h Planck's constant, and I_1^0/I_2^0 the intensity ratio of the two emission lines in the limit of zero Eu^{3+} concentration. The first term on the right of Eq. (4) describes the change in intensity ratio due to the depopulation of the two levels, while the second term takes into account the feeding of the first excited state from the second via the energy transfer to Eu^{3+} .

Along the same line of reasoning, an absolute increase in emission intensity I_1 is achieved when

$$Q_2 > \frac{Q_1}{1 - Q_1} \frac{I_1^0}{I_2^0} \frac{W_1}{W_{1r}} \frac{\nu_2}{\nu_1}. \quad (5)$$

Let us stress that in the ideal case of $S_1 = 0$ ($Q_1 = 0$) the analysis presented here is greatly simplified. The quenching

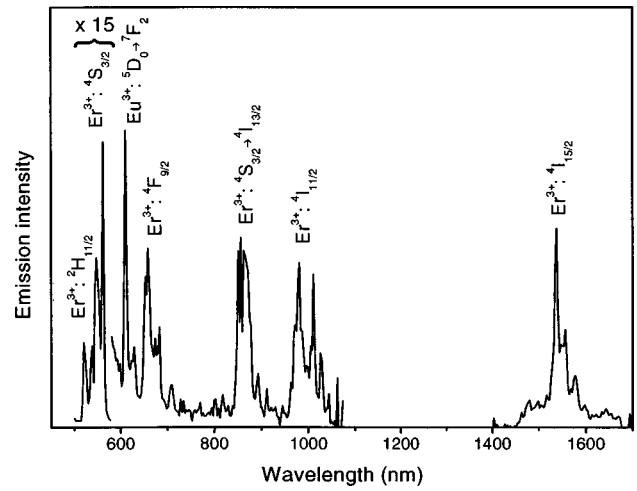


FIG. 2. Typical emission spectrum of an Er^{3+} and Eu^{3+} doped Y_2O_3 waveguide, excited at 488 nm. Where no final state for a transition is given, the excitation relaxes directly to the ground state of the relevant ion.

of the first excited state is very likely linked to the ion implantation, and can be reduced to zero using other doping methods (compare, e.g., Ref. 3).

B. Experimental results

Figure 2 shows the emission spectrum of the sample doped with 0.19 at. % erbium and 0.44 at. % europium in the visible and near infrared region, when excited at 488 nm. Emission lines of both Er^{3+} and Eu^{3+} can be identified, confirming the triply charged state of the ions in the matrix. The weaker emission of Eu^{3+} as compared to Er^{3+} is due to the small excitation cross section of Eu^{3+} at 488 nm. Figure 3 compares decay traces at 981 nm originating from the $\text{Er}^{3+} {}^4I_{11/2}$ level in Y_2O_3 with and without addition of 0.24 at. % europium. The decay is single exponential in the sample without europium, with a decay rate of 471 s^{-1} . Upon addition of europium, the decay becomes faster, the decay rate increases to 947 s^{-1} , and the decay becomes nonsingle ex-

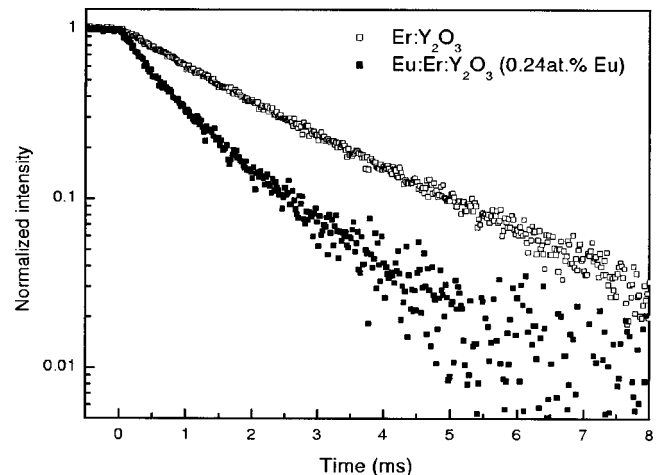


FIG. 3. Photoluminescence decay of the $\text{Er}^{3+} {}^4I_{11/2}$ state in Y_2O_3 monitored at 981 nm. The erbium concentration is 0.19 at. %. Decay traces are shown for a sample containing no europium and a sample containing 0.24 at. % europium.

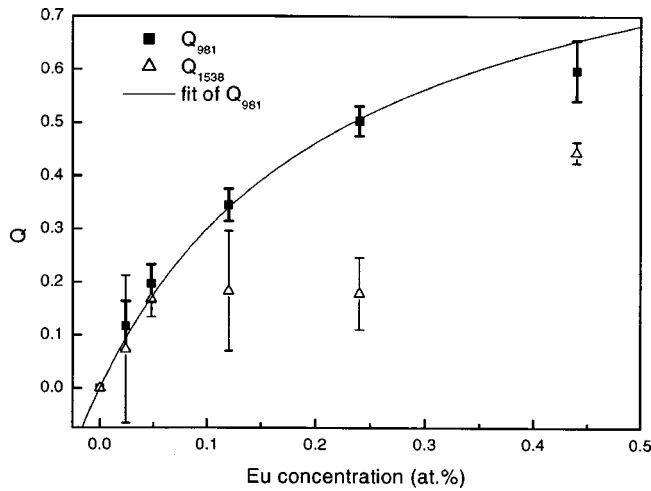


FIG. 4. Branching ratio of the $\text{Er}^{3+}(^4I_{11/2} \rightarrow ^4I_{13/2})$ to Eu^{3+} energy transfer (Q_{981}) and the fraction of energy lost from the $\text{Er}^{3+}:^4I_{13/2}$ state due to europium implantation (Q_{1538}). The line is a fit of Q_{981} to Eq. (2).

ponential. By evaluating decay rates from curves taken at 981 and 1538 nm, we obtain experimental values for the fraction of the population de-excited via a channel induced by the europium

$$Q_i^{N_q} = 1 - \frac{W_i^0}{W_i^{N_q}} \quad (6)$$

The index i labels the emission wavelength, the superscripts 0 and N_q refer to the europium concentration.

$Q_{1538}^{N_q}$ can be identified directly with Q_1 as given in the previous section, since the definition of the latter does not explicitly state a dependence on N_q . Conversely, if $Q_{981}^{N_q}$ exhibits the functional form of Q_2 , this is a clear indication that energy transfer towards Eu^{3+} really takes place.

In Fig. 4 we show the values for $Q_{1538}^{N_q}$ and $Q_{981}^{N_q}$ as a function of europium concentration. $Q_{981}^{N_q}$ increases monotonically and seems to saturate for high europium concentrations. $Q_{1538}^{N_q}$, however, increases for low europium concentrations, and saturates for intermediate europium concentrations. At $N_q = 0.44$ at. % we see another increase. Included in Fig. 4 is a fit of Eq. (2) to the data of $Q_{981}^{\text{exp}, N_q}$, with C_2 as the single free parameter. The data is reproduced well for an energy transfer coefficient C_2 of $2.9 \times 10^{-18} \text{ cm}^3/\text{s}$. This value is nearly an order of magnitude higher than the cooperative upconversion coefficient from the first excited state of Er^{3+} in Y_2O_3 ,⁹ indicating that the energy transfer towards europium is indeed efficient.

The data for $Q_{1538}^{N_q}$, on the other hand, cannot even be partially fitted to an equation of the form of Eq. (2), justifying the open definition of Q_1 . With these data we can exclude that the increase in decay rate of the $^4I_{13/2}$ level is caused by energy transfer to Eu^{3+} . Both resonant and phonon assisted energy transfer have the same dependency on N_q , and should therefore be reproduced by a function of the form of Eq. (2). This stands in clear contrast to our observations. Rather, we attribute the increase of the $^4I_{13/2}$ decay rate to quenching via implantation induced defects.

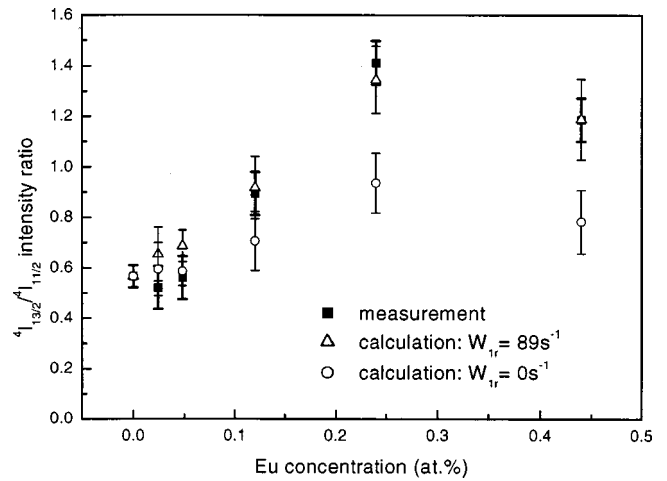


FIG. 5. Ratio of emission intensity from the $\text{Er}^{3+} \ ^4I_{13/2}$ and $^4I_{11/2}$ energy levels. Included are calculations according to equation 4 with $W_{1r} = 89$ and 0 s^{-1} .

It is clear from Fig. 4 that through the right choice of europium concentration, a substantial increase of the transition rate from the second to the first excited state of erbium can be induced at a low cost in lifetime of the first excited state itself.

For completeness let us state that we have also measured the change in decay rate of erbium energy levels in the visible region. A significant increase is observed only in the sample containing 0.44 at. % europium. In this case, the $^2H_{11/2}$ and $^4S_{3/2}$ levels are the only ones affected, with Q_{563} and Q_{521} amounting to 0.2 ± 0.1 . This may be due to nonresonant energy transfer to the $^5D_{0,1}$ levels of Eu^{3+} (cf. Fig. 1).

The validity of the model can be independently checked by measuring the intensity ratio of the emission originating from the $^4I_{13/2}$ and $^4I_{11/2}$ levels. Figure 5 shows these measurements as a function of europium concentration. The intensity ratio increases from 0.57 without europium to 1.41 at 0.24 at. % europium. A slightly lower value is observed at 0.44 at. % europium. Included in the figure are data calculated according to Eq. (4), with the data of Fig. 4 as input. The measurement is once again reproduced well by the calculation. The only free parameter here is the radiative decay rate of the first excited state W_{1r} , which has been adjusted to 89 s^{-1} for the best fit. As a comparison, the total decay rate W_1 was measured to be 115.7 s^{-1} .

To illustrate the effect of the increased branching ratio from the $^4I_{11/2}$ to the $^4I_{13/2}$ state, we have also plotted the calculated values for $W_{1r} = 0$. It is clear that for high europium concentrations the second term on the right-hand side of Eq. (4) contributes significantly to the intensity ratio. As stated earlier, this term represents the contribution caused by the additional feeding of the $^4I_{13/2}$ level via the interaction between the $^4I_{11/2}$ level and Eu^{3+} . It is only this term that contains the adjustable parameter W_{1r} . In case all europium-induced de-excitation of the $^4I_{11/2}$ state were towards the ground state, this term would be zero this is equivalent to setting $W_{1r} = 0$. The values of the first term of Eq. (4), however, lie significantly lower than the measurement points,

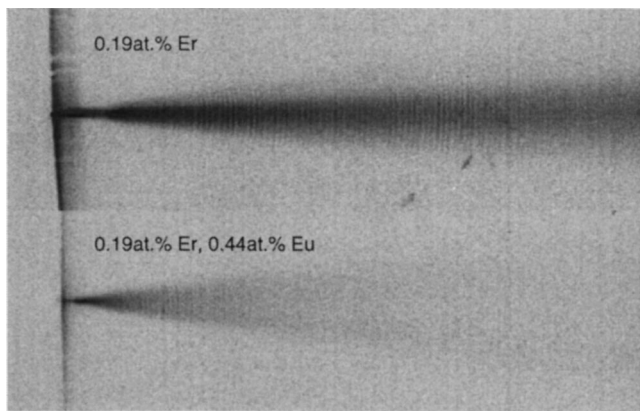


FIG. 6. False color image of the green emission of Er^{3+} with and without europium. The green emission from the $\text{Er}^{3+} {}^4S_{3/2}$ state is represented in black. 980 nm light is coupled into the planar waveguide from a fiber (left hand side of the images). In the presence of 0.44 at. % europium, the green upconversion emission is reduced considerably.

especially at high europium concentrations as shown in Fig. 5. Accordance can only be achieved by postulating the model detailed in the previous section. From the intensity ratios we can therefore exclude direct de-excitation of the ${}^4I_{11/2}$ level to the ground state via, e.g., defects.¹⁰

From the experimental data it follows that inequality 5 is fulfilled for Eu^{3+} concentrations between 0.1 and 0.3 at. %. Assuming that the rate equation model fully describes the physics in our samples, this means that in spite of the higher decay rate of the ${}^4I_{13/2}$ state, in this region absolute intensity enhancement is achieved. For the sample with the highest Eu^{3+} concentration, this is not any more the case, since the increase of the decay rate of the ${}^4I_{13/2}$ state is too high. This problem might be overcome by using a doping method other than ion implantation, which does not affect the decay rate of the ${}^4I_{13/2}$ state.

Two of the great loss mechanisms of excitation in integrated optical amplifiers are cooperative upconversion and excited state absorption. These two processes are enhanced by population buildup in an excited state. Increasing the decay rate of the second excited state of erbium should therefore decrease the green emission due to upconversion processes originating from this state. Figure 6 compares optical images of planar waveguides doped with 0.19 at. % erbium, one of them codoped with 0.44 at. % europium. Excitation takes place by coupling 979 nm radiation into the waveguide from a fiber (left side of the images). The excitation power was adjusted such that the emission at 1538 nm, a measure for the population of the ${}^4I_{13/2}$ level, had the same intensity for both measurements. The green emission due to upconversion is clearly reduced on codoping with europium.

The reduction of upconversion emission due to codoping with Eu^{3+} can also find application in erbium-doped amplifiers pumped directly into the ${}^4I_{13/2}$ level, e.g., with 1480 nm light. In highly doped amplifiers, cooperative upconversion and excited state absorption from the ${}^4I_{13/2}$ state lead to a significant population of the ${}^4I_{11/2}$ level. The same mechanisms of gain reduction as described for 980 nm pumping

come into effect, on a somewhat lesser scale. Even in such a system it is therefore desirable to increase the transition rate between the ${}^4I_{11/2}$ and ${}^4I_{13/2}$ states.

IV. CONCLUSION

The population in the first excited state of Er^{3+} in an Y_2O_3 matrix under excitation at 980 nm can be increased by codoping with Eu^{3+} . This is due to a controlled resonant energy transfer from the second excited state of Er^{3+} towards Eu^{3+} , reducing the population in that state in favor of the population in the first excited state. This process of selective increase of the decay rate of a certain energy level with control over the transition's final state is especially useful for materials with low phonon energies.

We have been able to show that energy transfer between Er^{3+} and Eu^{3+} is responsible for the acceleration of the decay of the erbium's second excited state in Y_2O_3 doped by ion implantation. By codoping with only 0.44 at. % europium we have achieved a 60% efficiency of the energy transfer in depopulating the second excited state. This is reflected in the emission intensities: the emission from the first excited state is significantly increased for europium concentrations above 0.1 at. %. The reduced population of the second excited state leads further to a decrease in green upconversion photoluminescence under 980 nm excitation. In this way an important loss channel in highly pumped optical amplifiers can be effectively closed.

ACKNOWLEDGMENTS

H. J. van Weerden and P. V. Lambeck are gratefully acknowledged for providing the Y_2O_3 films. This work is part of the research program of FOM, and was financially supported by NWO and IOP Electro-Optics.

¹B. Simondi-Teisseire, B. Viana, D. Vivien, and A. M. Lejus, *Opt. Mater.* **6**, 267 (1996).

²A.-F. Obaton, J. Bernard, C. Parent, G. Le Flem, C. Labbé, P. Le Boulanger, and G. Boulon, *Eur. Phys. J.: Appl. Phys.* **4**, 315 (1998).

³Z. Meng, T. Yoshimura, Y. Nakata, N. J. Vasa, and T. Okada, *Jpn. J. Appl. Phys., Part 2* **38**, L1409 (1999).

⁴A. A. Andronov, I. A. Grishin, V. A. Gur'ev, V. V. Orekhovskii, and A. P. Savikin, *Tech. Phys. Lett.* **24**, 365 (1998).

⁵H. J. van Weerden, T. H. Hoekstra, P. V. Lambeck, and T. J. A. Popma, in *Proceedings of the 8th European Conference on integrated optics*, Stockholm, Sweden (1997) p. 169.

⁶T. H. Hoekstra, PhD thesis, University of Twente, The Netherlands, March 1994.

⁷N. C. Chang and J. B. Gruber, *J. Chem. Phys.* **41**, 3227 (1964).

⁸N. Yamada, S. Shionoya, and T. Kushida, *J. Phys. Soc. Jpn.* **32**, 1577 (1972).

⁹E. RADIUS, Master thesis, University of Amsterdam, The Netherlands, June 1994.

¹⁰Actually the argument has to be revised slightly. Assuming an additional de-excitation channel proportional to N_q , leading from the ${}^4I_{11/2}$ level to the ground state, will change the dependencies on europium concentration of neither Q_2 nor the intensity ratio. The parameter arrived at in Fig. 5 then constitutes a lower limit for W_{1r} rather than W_{1r} itself. On the other hand, the measured lifetime of the ${}^4I_{13/2}$ state extrapolated to zero erbium concentration [96 s^{-1} (Ref. 6)] provides an upper limit for W_{1r} . Since the radiative decay rate has not been determined independently, we have to conclude by pointing out that the limits to W_{1r} do not allow for enough variation to jeopardize the statements made in the main text.